HAL open science

Automated approach for source location in shallow water

Angèle Niclas, Josselin Garnier

To cite this version:

Angèle Niclas, Josselin Garnier. Automated approach for source location in shallow water. WAVES 2024 - The 16th International Conference on Mathematical and Numerical Aspects of Wave Propagation, Jun 2024, Berlin, France. hal-04712223

HAL Id: hal-04712223

https://hal.science/hal-04712223v1

Submitted on 27 Sep 2024

HAL is a multi-disciplinary open access archive for the deposit and dissemination of scientific research documents, whether they are published or not. The documents may come from teaching and research institutions in France or abroad, or from public or private research centers.

L'archive ouverte pluridisciplinaire **HAL**, est destinée au dépôt et à la diffusion de documents scientifiques de niveau recherche, publiés ou non, émanant des établissements d'enseignement et de recherche français ou étrangers, des laboratoires publics ou privés.

Automated approach for source location in shallow water

Angèle Niclas[1,*], **Josselin Garnier**[2]
[1]MAP5, CNRS, Université Paris Cité, Paris, France
[2]CMAP, CNRS, École polytechnique, Institut Polytechnique de Paris, Palaiseau, France
*Email: angele.niclas@math.cnrs.fr

Abstract

This work proposes a fully automated method for recovering the location of a source and medium parameters in shallow water. The scenario involves an unknown source emitting low-frequency sound waves in a shallow water environment and a single hydrophone recording the signal. Using the spectrogram of each modal component obtained by a warping method, we investigate how to recover the modal travel times and we provide stability estimates. A penalized minimization algorithm is then presented to estimate the source location and medium parameters. The proposed method is tested on different experimental data, demonstrating its effectiveness in real-world scenarios.

Keywords: Source location, Spectrogram analysis, Shallow water, Inverse problems

1 Introduction

In this study, we work with time signals emitted by a broadband source and recorded by a single hydrophone in a shallow water environment. We aim to recover the distance between the source and the receiver and relevant medium parameters. While several manual methods have been proposed previously (see a review in [1]), they suffer from high dependency on user expertise and lack rigorous mathematical justification.
Here, we develop an automated approach, eliminating manual intervention and accelerating the process. Moreover, we provide rigorous mathematical proofs for the convergence of our algorithm to ensure the robustness and reliability of the estimation outcomes.

2 Wave propagation in shallow water

We model the shallow water environment by a Pekeris waveguide $\mathbb{R} \times (-\infty, 0)$ with a water layer of depth D, celerity c_{w} and density ρ_{w}, and an infinite sediment layer with celerity c_{b} and density ρ_{b} (see more details in [2]). A broadband source at $(0, z_s)$ emits a signal $u(t)$, and a single hydrophone records this signal at (r, z_r). For a frequency $\omega \in \mathbb{R}^+$, the analysis conducted in [1] demonstrates that if $r \gg c_{\mathrm{w}}/\omega$ then

$$\hat{u}(\omega) = \sum_{n=1}^{N} \hat{u}_n(\omega), \ \hat{u}_n(\omega) = \frac{A_n(\omega) e^{irk_n(\omega)}}{\sqrt{rk_n(\omega)}}, \quad (1)$$

where $\hat{u}$ is the Fourier transform of u, N is the number of propagative modes and k_n is the wavenumber defined in [2]. Through the warping method detailed in [2], we can precisely retrieve each modal component $\hat{u}_n$.

3 Spectrograms

Given the unknown nature of z_s and thus A_n, the retrieval of the different parameters requires the use of the phases of individual modal components. However, traditional phase recovery encounters challenges in noisy environments. We adopt an alternative approach to overcome this limitation by employing a time-frequency representation known as the spectrogram. For each n, the spectrogram is defined as follows:

$$S_n(t, \omega) = \left| \int_{\mathbb{R}} \hat{u}_n(\omega + \xi) e^{-\frac{\xi^2}{2\sigma^2}} e^{i\xi t} \mathrm{d}\xi \right|. \quad (2)$$

The aspect of the spectrogram depends on the choice of the parameter σ, as illustrated in Figure 1. Using an approximation of the stationary phase, we can prove that

$$S_n(t, \omega) \approx |A_n(\omega)|^2 \frac{\sigma^2}{2\pi} e^{-\sigma^2 (t - t_n(\omega))^2}. \quad (3)$$

Here, $t_n(\omega) = rk_n'(\omega)$ represents the modal travel time, and the energy of the spectrogram concentrates along the curves $\omega \mapsto t_n(\omega)$, as depicted in Figure 1.

4 Reconstruction of modal travel times

For a fixed n, we aim at approaching the curve t_n given the spectrogram $S_n(t, \omega)$, and we consider a signal of the form $u_n(t) + B(t)$ where $B(t)$ is a Gaussian additive noise satisfying $\mathbb{E}(B(t)) = 0$ and

$$\mathrm{Cov}\left(B(t), B(t')\right) = \delta^2 e^{-\frac{(t-t')^2)}{2T_\delta^2}}. \quad (4)$$

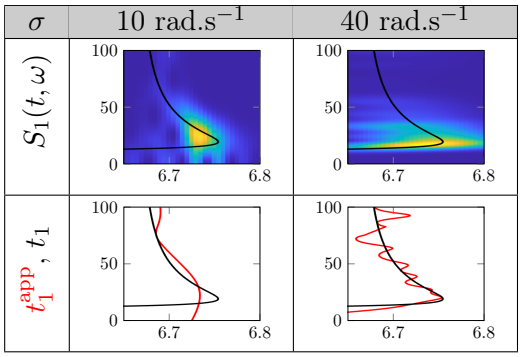

Figure 1: $S_1(t,\omega)$ for two values σ on synthetical data, the recovered curve $\omega \mapsto t_1^{\text{app}}(\omega)$ (red) and the theoretical curve $\omega \mapsto t_1(\omega)$ (black).

This noise model proves to be a reliable approximation for both measurement and environmental noise. Using the received signal, the standart deviation δ and the characteristic time-scale T_δ can be estimated. To recover t_n from the spectrogram using the approximation (3), various methods detailed in [3] can be employed. Here, we choose the maximum method for its simplicity and robustness, and we introduce

$$\forall \omega \in \mathbb{R}^+ \quad t_n^{\text{app}}(\omega) = \text{argmax}_{t\in\mathbb{R}} S_n(t,\omega). \quad (5)$$

Using the cut-off frequency of the mode n denoted by $\omega_{c,n}$ [1], we quantify the error between t_n and t_n^{app} in noisy settings:

Theorem 1 *Defining $\sigma_{lim}(\omega) = \omega_{c,n}/3 - \omega/4$ (which do not depend on δ, T_δ, σ), we have*

$$\mathbb{E}(|t_n^{app}(\omega) - t_n(\omega)|) \leq$$
$$C_1 + C_2 \mathbf{1}_{\sigma>\sigma_{lim}} + C_3\sigma + C_4 \delta T_\delta^{1/2} \sigma^{-3/2}. \quad (6)$$

This quantity is minimal when $\sigma = \sigma_{opt}$, where

$$\sigma_{opt}(\omega) \in \left\{\sigma_{lim}(\omega),\, C_5 \delta^{2/5} T_\delta^{1/5}\right\}. \quad (7)$$

Here, all quantities C_i are explicit and can be computed using the recorded signal u.

We see here that one needs to test the two values in (7) to determine which one provides the minimal error. However, the most common situation seems to be the one where $\sigma_{\text{opt}} = \sigma_{\text{lim}}$ and we now choose this setting, illustrated in Figure 2 for experimental data.

5 Parameter reconstruction

We now aim to recover the different parameters of interest. The usual approach, as described in [1], involves minimizing the non-convex functional

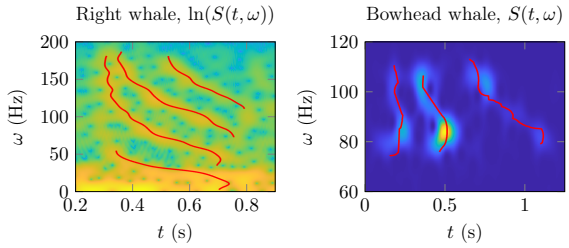

Figure 2: $S(t,\omega)$ and recovered curves $\omega \mapsto t_n^{\text{app}}(\omega)$ (red) with the choice $\sigma = \sigma_{\text{opt}}$ for experimental data of right whale gunshot and bowhead whale upsweep [1].

$$J(r, c_w, c_b, \rho_w, \rho_b, D, dt) =$$
$$\|t_n(r, c_w, c_b, \rho_w, \rho_b, D) - dt - t_n^{\text{app}}\|_{\ell^2}^2. \quad (8)$$

However, optimizing J can be computationally expensive, and the minimum may be found at non-physical values. To address these challenges, we propose a Bayesian approach incorporating prior knowledge of specific parameters denoted as ρ_{w}^0, ρ_{b}^0, c_{w}^0, and D^0. Accounting for the trust in these parameters, we minimize the new functional

$$\tilde{J} = J + \alpha\Big(\left|(D^0 - D)/D^0\right|^2 + \left|(\rho_{\text{b}}^0 - \rho_{\text{b}})/\rho_{\text{b}}^0\right|^2$$
$$+ 10\left|(\rho_{\text{w}}^0 - \rho_{\text{w}})/\rho_{\text{w}}^0\right|^2 + 10\left|(c_{\text{w}}^0 - c_{\text{w}})/c_{\text{w}}^0\right|^2\Big), \quad (9)$$

where α is chosen so that the penalization part is of the same order as J. The modified functional $\tilde{J}$ is now convex and computationally efficient to minimize. We have successfully tested this Bayesian approach on both synthetic and experimental data. The results, presented in Table 1, demonstrate a significant enhancement in performance, particularly for parameters lacking prior knowledge, such as r and c_b.

Relative error	r	c_b	r [1]	c_b [1]
Synthetical data	<1 %	<1 %	3%	8%
Right whale [1]	<1%	3%	6%	14%
Bowhead whale [1]	4%	9%	10%	21%

Table 1: Relative reconstruction errors: minimization of (9) with $\sigma = \sigma_{\text{opt}}$ compared with the method [1].

References

[1] J. Bonnel et al, Nonlinear time-warping made simple, *J. Acoust. Soc. Am.* **147(3)** (2020), pp. 1897–1926.

[2] A. Niclas and J. Garnier, Automated approach for recovering modal components in shallow water, *submitted*, arXiv: 2307.15491.

[3] S. Meignen et al, On demodulation for multicomponent signals, *IEEE Trans. Signal Process.* **65(8)** (2017), pp. 2093–2103.